

Aberration-free short focal length x-ray lenses

LUCIA ALIANELLI,^{1,*} MANUEL SÁNCHEZ DEL RIO,² OLIVER J. L. FOX,^{1,3} AND KATARZYNA KORWIN-MIKKE⁴

¹Diamond Light Source Ltd., Chilton, Didcot OX11 0DE, UK

²European Synchrotron Radiation Facility, BP 220 38043 Grenoble Cedex, France

³School of Chemistry, University of Bristol, Bristol BS8 1TS, UK

⁴Oxford Instruments Plasma Technology, Yatton BS49 4AP, UK

*Corresponding author: lucia.alianelli@diamond.ac.uk

Received 2 June 2015; revised 23 July 2015; accepted 24 July 2015; posted 10 September 2015 (Doc. ID 241809); published 25 November 2015

We treat the problem of defining the ideal x-ray refractive lens design for point focusing of low emittance x-ray beams at third- and fourth-generation synchrotron sources. The task is accomplished by using Fermat's principle to define a lens shape that is completely free from geometrical aberrations. Current microfabrication resolution limits are identified, and a design that tolerates the inherent fabrication imperfections is proposed. The refractive lens design delivers nanometer-sized focused x-ray beams and is compatible with current microfabrication techniques. © 2015 Optical Society of America

OCIS codes: (080.0080) Geometric optics; (220.0220) Optical design and fabrication; (340.0340) X-ray optics.

<http://dx.doi.org/10.1364/OL.40.005586>

X rays are weakly refracted by most materials, and yet refractive and refractive-diffractive (or kinoform) lenses are some of the most promising nanofocusing optics for beam lines at third- and fourth-generation synchrotron laboratories. Collimating or focusing lenses are often preferred to other optics that deliver higher flux (e.g., bent mirrors or multilayers) in cases such as crystal diffraction experiments, imaging, and small-angle scattering, where intrinsic chromaticity is not a limitation to the experimental technique. Simple alignment, small lens footprint, and the absence of zero or higher orders of diffraction make these lenses even more attractive.

Nanofocusing optics have very short focal lengths, and, for grazing incidence mirrors, this implies a limited mirror length and beam acceptance. Micro-optics, such as zone plates, multilayer-Laue lenses, and refractive lenses, have even smaller acceptance than mirrors because limited aspect ratios are possible with the fabrication methods currently employed. Planar nanofocusing refractive lenses have been made using e-beam or x-ray beam lithography and silicon etching [1–3] or diamond chemical vapor deposition (CVD) [4]. Single crystal silicon substrates have been successfully used to fabricate lenses that are installed on scanning microscope beam lines. Development of a robust method for fabricating diamond x-ray refractive optics is, thus, a high-priority research topic in the general field of synchrotron optics and instrumentation [5,6]. A single crystal diamond is

the ideal x-ray lens material due to both its excellent thermal properties (e.g., on free-electron laser beams [7,8]) and low x-ray absorption. However, microfabrication of diamond is not currently as advanced as silicon due to the material hardness and chemical inertness. Nanoprobe beam lines, which are often equipped with low-aperture optics, would enormously benefit from diamond lenses with higher efficiency. In this Letter, we propose advanced lens designs for silicon and diamond optics.

The theoretical problem of finding the ideal nanofocusing x-ray lens design has been discussed [9]. To increase the numerical aperture, while removing geometrical aberrations, arrays of N lenses with decreasing radii have to be used [9,10]. The explicit analytical solutions for such aberration-free arrays have not been previously presented. Finally, Fermat's principle has been used to define a lens shape that is not affected by geometric aberrations [11], and, for highly collimated beams such as x rays from synchrotron sources, this shape is either an ellipse or a hyperbola. In the paraxial rays approximation, the focal length of a refractive surface is given by

$$f_i = \frac{R_i}{\delta}, \quad i = 1, 2, 3, \dots, N, \quad (1)$$

where R_i is the curvature radius at the apex, and δ is the real part of the refractive-index decrement n :

$$\delta = 1 - RE(n), \quad (2)$$

For x rays, δ is a very small positive number. A hypothetical single surface nanofocusing lens would require a radius of curvature that is too small for existing fabrication technologies. It is, therefore, necessary to define geometrical properties of an aberration-free optic consisting of an array of N refractive surfaces in which $R_i < R_{i-1}$.

We start from some simple observations on the nature of aberration-free x-ray refractive surfaces [11,12]:

1. An elliptical surface will focus a parallel x-ray beam incident upon it as the radiation passes from the material into air.
2. A hyperbolic surface will focus a parallel x-ray beam incident upon it as the radiation passes from air into the material.
3. An oval of Descartes will focus an incident divergent beam emitted by a point source.
4. There is no analytical solution for a lens shape to refocus an incident convergent beam.

Therefore, an array of N refractive surfaces, where each subsequent surface focuses the radiation with higher angles of convergence, i.e., to shorter back focal lengths [12], does not exist. Similarly, a convergent beam from the first surface in the array cannot be focused further by a second one. The only analytically correct, aberration-free solution for the second refractive surface is a collimating optic. The third surface is then focusing the incoming parallel beam. This sequence can be repeated, and, in general, odd-numbered surfaces will be focusing the beam; even-numbered lenses will be collimating the radiation. In an array of refractive surfaces, the back focal length is defined as the distance of the focal plane from the apex of the last surface in the array, which is calculated for a parallel incident beam [12]. The lens-maker formula for thick lenses can be used to determine the back focal length $\bar{f} \equiv \bar{f}_N$ of the compound system:

$$\bar{f} = \left(\frac{1}{\bar{f}_{N-1}} - \frac{1}{d_{N-1} - f_N} \right)^{-1}. \quad (3)$$

The back focal length of an array with a total number i of refractive surfaces, where d_i is the separation from lens apex $i - 1$ to lens apex i , is

$$\bar{f}_i = \left(\frac{1}{\bar{f}_{i-1}} - \frac{1}{d_{i-1} - f_i} \right)^{-1}. \quad (4)$$

For numerical simulation purposes, the designer can verify that each surface produces an image, at distance q_i from the lens apex, defined by

$$q_i = \left(\frac{1}{f_i} - \frac{1}{p_i} \right)^{-1}. \quad (5)$$

The object distance for any surface with $i \geq 2$ is

$$p_i = (d_{i-1} - q_{i-1}). \quad (6)$$

The lengths of the refractive elements are not negligible compared with their respective focal lengths; therefore, Eqs. (5) and (6) have to be applied to each surface and not to the compound system. The theoretically correct lens systems are illustrated in Fig. 1. These aberration-free arrays are made of

1. N elliptical surfaces
2. $N/2$ ellipses (for odd values of i) and $N/2$ hyperbolas (for even values of i)

3. N hyperbolic surfaces
4. $N - 1$ hyperbolic surfaces with a final elliptical surface

All arrays in the figure are, in principle, equivalent; however, they are not all practically feasible due to length of the array. An array with nested lenses [Fig. 1(a)] is therefore the best solution.

Due to absorption, we propose the use of kinoform lens arrays [10], also shown in Fig. 2. As discussed, it may not be possible to precisely sculpt a kinoform diamond lens; therefore, a diamond ultrashort focal lens is illustrated in Fig. 3. In order to describe a possible nanofocusing-nested kinoform lens, we choose a back focal length of the compound system with $\bar{f} = 21$ mm, $N = 3$. Design parameters and efficiency calculations, including the diffraction limit or smallest focused beam size s , are summarized in Tables 1 and 2. We use ray tracing to simulate single ellipse lenses and arrays on a typical focusing setup on a high brilliance undulator source. The results show that the proposed designs are capable of focusing light to a nanometer-sized beam; therefore, the focusing is diffraction limited.

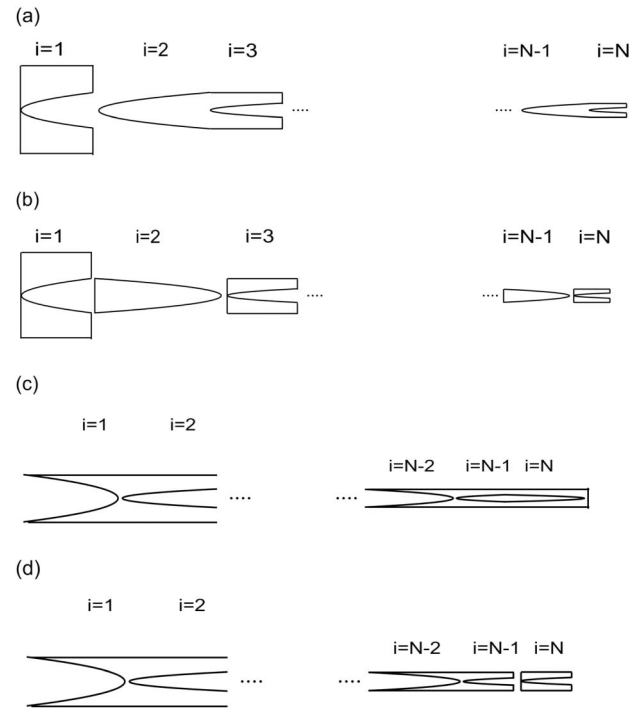


Fig. 1. (a) Arrays of elliptical surfaces. (b) Alternating elliptical and hyperbolic surfaces. (c) Hyperbolic surfaces. (d) Hyperbolic surfaces with one final elliptical surface.

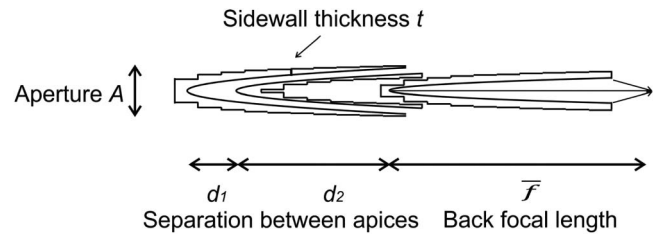


Fig. 2. Design for a silicon or diamond lens with kinoform profiles (see Tables 1 and 2 for efficiency calculations).

For the silicon kinoform lenses, a smallest sidewall width is proposed of $t = 1 \mu\text{m}$ (Table 1); for diamond, we use $t = 10 \mu\text{m}$ (Table 2). This is due to the aforementioned limitations of diamond microfabrication and lower aspect ratio expected for this material. Lens transmission, T , is calculated as the ratio of flux transmitted to flux incident within the lens effective aperture, A_{eff} [13]. The effective aperture is defined as the aperture in which the transmitted flux is 75% of the total maximum flux delivered by the lens, in its full geometrical aperture, A . The lens design provides a solution for aberration-free, diffraction-limited focusing when the incident beam is collimated. The diffraction limited beam size, s , is calculated as the full width at half-maximum of the Airy disk:

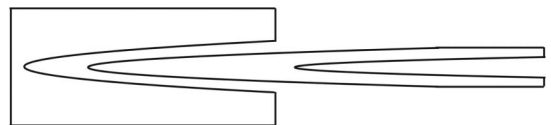


Fig. 3. Design for a diamond lens without kinoform profiles.

Table 1. Calculated Properties of a Kinoform Silicon Lens Array Where $N = 3$, $\bar{f} = 21$ mm, $t = 1$ μ m

E [keV]	8	10	12	14	16	18	20
R_1 [μ m]	0.770	0.492	0.338	0.248	0.189	0.149	0.121
R_2 [μ m]	0.762	0.487	0.335	0.245	0.188	0.148	0.120
R_3 [μ m]	0.17	0.108	0.074	0.0545	0.042	0.033	0.027
A [μ m]	150	160	140	130	100	95	85
A_{eff} [μ m]	43	28	55	59	55	56	54
T [%]	17	23	28	31	33	35	36
s [nm]	57	71	29.5	24	22	19.5	18

Table 2. Calculated Properties of a Kinoform Diamond Lens Array Where $N = 3$, $\bar{f} = 21$ mm, $t = 10$ μ m

E [keV]	8	10	12	14	16	18	20
R_1 [μ m]	1.14	0.727	0.505	0.371	0.284	0.224	0.182
R_2 [μ m]	0.13	0.72	0.5	0.367	0.281	0.222	0.180
R_3 [μ m]	0.250	0.160	0.11	0.082	0.062	0.049	0.040
A [μ m]	180	140	110	100	88	110	100
A_{eff} [μ m]	58	62	60	59	55	64	60
T [%]	39.5	40.4	41	41	41	41.5	41.5
s [nm]	42	31.5	27	24	22	17	16

$$s = 0.75 \times \frac{\lambda}{2 \times NA}, \quad (7)$$

where λ is the photon wavelength, and NA is the numerical aperture:

$$NA = \frac{A_{\text{eff}}}{2\bar{f}}. \quad (8)$$

One important property of an aberration-free lens is that the focused beam waist is found at the nominal focal plane, i.e., at distance \bar{f} from the apex of the last surface (when the beam impinging on the last surface is collimated). The geometrical ray-tracing results illustrating this fact are shown in Fig. 4. We have used an ideal single ellipse or array of ellipses [Fig. 1(a) and Table 1, $E = 8$ keV] and simulated focusing of an incoming beam with divergence $\sigma' = 1$ μ rad [Fig. 4(a)] and

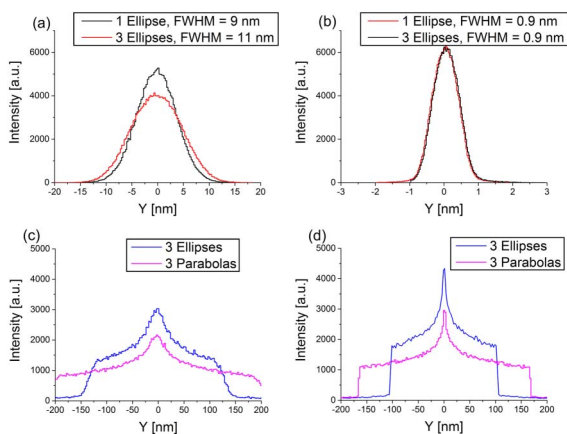


Fig. 4. Ray-tracing simulations [14] lens system with nominal focal length $\bar{f} = 21$ mm: (a), (c) with an incident beam divergence $\sigma' = 1$ μ rad and (b), (d) $\sigma' = 0.01$ μ rad; a system with no aberration as described in Fig. 1(a) and Table 1, in (a) and (b); a system of three refractive surfaces with decreasing radii (however, not using the design recommended in this Letter) in (c) and (d). In all cases, the lens aperture is $A = 40$ μ m.

$\sigma' = 0.01$ μ rad [Fig. 4(b)]. Only geometrical focusing is considered, i.e., no diffraction is present. We have used arrays of ellipses or parabolas with decreasing radii, however, not following the optimal design, for Figs. 4(c) and 4(d) (with an incoming beam with divergence $\sigma' = 1$ μ rad and $\sigma' = 0.01$ μ rad respectively). The lens focal plane is found almost exactly at $\bar{f} = 21$ mm in both cases (a) and (b). Large aberrations are present in both cases (c) and (d), and the beam waist is found several mm away from the nominal focal plane.

In conclusion, we have offered a simple yet analytically correct design for planar nanofocusing refractive optics. We have shown that they can be designed with improved apertures. Silicon x-ray lenses are not currently available commercially; however, the fabrication tools exist to make them a standard beam line optics component. Several fabrication methods are being tested for achieving similar results in diamond, including molding, laser cutting, and dry etching. We have shown that higher apertures and transmission values are possible with this desirable material, in addition to a smaller focused beam of order $s \approx 20$ nm, thereby justifying the trend in diamond research for optics synchrotron applications.

In practical terms, the lens radii required in these designs are at the limit of current lithographic techniques. We have tested fabrication of a silicon kinoform lens with a radius as small as few tens of nanometers. Fabrication was made using e-beam lithography and fast-switching Bosch deep reactive ion etching. The system employed was an Oxford Instruments PlasmaPro 100 Estrelas. Etch angles of approximately 89.9° and scalloping amplitudes lower than 40 nm were achieved.

Funding. Science and Technology Facilities Council (STFC) (ST/F001665/1) Facility Development Grant.

REFERENCES

1. C. G. Schroer, O. Kurapova, J. Patommel, P. Boye, J. Feldkamp, B. Lengeler, M. Burghammer, C. Riekel, L. Vincze, A. van der Hart, and M. Küchler, Appl. Phys. Lett. **87**, 124103 (2005).

2. K. Evans-Lutterodt, J. M. Ablett, A. Stein, C. Kao, D. Tennant, F. Klemens, A. Taylor, C. Jacobsen, P. Gammel, H. Huggins, G. Bogart, S. Ustin, and L. Ocola, *Opt. Express* **11**, 919 (2003).
3. L. Alianelli, K. J. S. Sawhney, R. Barrett, I. Pape, A. Malik, and M. C. Wilson, *Opt. Express* **19**, 11120 (2011).
4. O. J. L. Fox, L. Alianelli, A. M. Malik, I. Pape, P. W. May, and K. J. S. Sawhney, *Opt. Express* **22**, 7657 (2014).
5. A. F. Isakovic, A. Stein, J. B. Warren, S. Narayanan, M. Sprung, A. R. Sandy, and K. Evans-Lutterodt, *J. Synchrotron Radiat.* **16**, 8 (2009).
6. M. Polikarpov, I. Snigireva, J. Morse, V. Yunkin, S. Kuznetov, and A. Snigirev, *J. Synchrotron Radiat.* **22**, 23 (2015).
7. C. David, S. Gorelick, S. Rutishauser, J. Krzywinski, J. Vila-Comamala, V. A. Guzenko, O. Bunk, E. Färm, M. Ritala, M. Cammarata, D. M. Fritz, R. Barrett, L. Samoylova, J. Grünert, and H. Sinn, *Sci. Rep.* **1**, 57 (2011).
8. D. Nilsson, A. Holmberg, H. Sinn, and U. Vogt, *AIP Conf. Proc.* **1365**, 120 (2011).
9. C. G. Schroer and B. Lengeler, *Phys. Rev. Lett.* **94**, 054802 (2005).
10. K. Evans-Lutterodt, A. Stein, J. M. Ablett, N. Bozovic, A. Taylor, and D. M. Tennant, *Phys. Rev. Lett.* **b**, 134801 (2007).
11. M. Sánchez del Rio and L. Alianelli, *J. Synchrotron Radiat.* **19**, 366 (2012).
12. E. Hecht, *Optics*, 4th ed. (Addison-Wesley, 2002).
13. W. Jark, F. Pérennès, and M. Matteucci, *J. Synchrotron Radiat.* **13**, 239 (2006).
14. C. Welna, G. J. Chen, and F. Cerrina, *Nucl. Instrum. Methods Phys. Res. Sect. A* **347**, 344 (1994).